Ain Shams Engineering Journal (2014) 5, 759–774

Ain Shams University

Ain Shams Engineering Journal

www.elsevier.com/locate/asej
www.sciencedirect.com

ELECTRICAL ENGINEERING

Automatic generation control with thyristor controlled series compensator including superconducting magnetic energy storage units

Saroj Padhan, Rabindra Kumar Sahu *, Sidhartha Panda

Department of Electrical Engineering, Veer Surendra Sai University of Technology (VSSUT), Burla 768018, Odisha, India

Received 7 February 2014; revised 19 March 2014; accepted 26 March 2014
Available online 16 May 2014

KEYWORDS

Automatic Generation Control (AGC);
Fuzzy logic controller;
Differential Evolution (DE) algorithm;
Thyristor Controlled Series Compensator (TCSC);
Superconducting Magnetic Energy Storage (SMES)

Abstract In the present work, an attempt has been made to understand the dynamic performance of Automatic Generation Control (AGC) of multi-area multi-units thermal–thermal power system with the consideration of Reheat turbine, Generation Rate Constraint (GRC) and Time delay. Initially, the gains of the fuzzy PID controller are optimized using Differential Evolution (DE) algorithm. The superiority of DE is demonstrated by comparing the results with Genetic Algorithm (GA). After that performance of Thyristor Controlled Series Compensator (TCSC) has been investigated. Further, a TCSC is placed in the tie-line and Superconducting Magnetic Energy Storage (SMES) units are considered in both areas. Finally, sensitivity analysis is performed by varying the system parameters and operating load conditions from their nominal values. It is observed that the optimum gains of the proposed controller need not be reset even if the system is subjected to wide variation in loading condition and system parameters.

1. Introduction

Load Frequency Control (LFC) is a very important issue in modern power system operation and control for supplying sufficient and reliable electric power with good quality. The main goal of the LFC is to maintain the system frequency of each area and the tie line power within tolerable limits with variation in load demands [1]. For power balance, the power generated should match with the total load demanded and associated system losses. However the load demands fluctuate randomly causing a mismatch in the power balance and thereby deviations in the area frequencies and tie-line powers from their respective scheduled values, called Automatic Load Frequency Control (ALFC) [2,3]. Due to the complexity of the modern power system, superior intelligent control design is essential. Literature study reveals that several control strategies have been proposed by many researchers over the past decades for LFC of power system. Many control and optimization techniques such as classical, optimal, Genetic Algorithm (GA), Particle Swarm Optimization (PSO), Fuzzy Logic Controller (FLC), and Artificial Neural Network (ANN), have been proposed for LFC [4–9]. Design of a controller for

* Corresponding author. Tel.: +91 9439702316.
E-mail addresses: callsaroj201@rediffmail.com (S. Padhan), rksahu123@gmail.com (R.K. Sahu), panda_sidhartha@rediffmail.com (S. Panda).

Peer review under responsibility of Ain Shams University.

Production and hosting by Elsevier

2090-4479 © 2014 Production and hosting by Elsevier B.V. on behalf of Ain Shams University.
http://dx.doi.org/10.1016/j.asej.2014.03.011

AGC can be divided into two groups. In the 1st group the controller gains are tuned by a suitable optimization algorithm. In the 2nd group researchers have adopted self-tuning techniques with the help of neural network and fuzzy logic. Fuzzy logic controllers have been successfully used for analysis and control of non-linear system in the past decades. Yesil et al. [10] have used a self-tuning fuzzy PID type controller for load frequency control of a two-area interconnected system. Khuntia and Panda [11] have used ANFIS approach for AGC of a three area system. Ghosal [8] have used PSO optimization technique to optimize the PID controller gain for a fuzzy based LFC. These methods provide good performances but the transient responses are oscillatory in nature. Fuzzy logic based PID controller can be successfully used for all non-linear system but there is no specific mathematical formulation to decide the proper choice of fuzzy parameters (such as inputs, scaling factors, membership functions, and rule base). Normally these parameters are selected by using certain empirical rules and therefore may not be the optimal parameters. Improper selection of input–output scaling factor may affect the performance of FLC to a greater extent.

To get an accurate insight into the AGC problem, it is necessary to include the important physical constraints in the system model. The major physical constraints that affect the power system performance are Generation Rate Constraint (GRC) and time delay. The Flexible AC Transmission System (FACTS) controllers [12] play a crucial role to enhance power system stability in addition to control the power flow in an interconnected power system. Several studies have explored the potential of using FACTS devices for better power system control since it provides more flexibility. A Superconducting Magnetic Energy Storage (SMES) is capable of controlling both active and reactive power simultaneously. SMES unit with small storage capacity can be essential not only as a fast energy compensation device for power consumptions of large loads, but also as a stabilizer of frequency oscillations [13]. TCSC is one of the FACTS controller which is enhanced the power system dynamics, power transfer capability of transmission lines and dynamic stability [14].

It obvious from the literature survey that the performance of the power system not only depends on the controller structure but also depends on the artificial optimization technique. Hence, proposing and implementing new high performance heuristic optimization algorithms to real world problems are always welcome. Differential Evolution (DE) is a population-based direct search algorithm for global optimization capable of handling non-differentiable, non-linear and multimodal objective functions, with few, easily chosen, control parameters [15,16]. However, the success of DE in solving a specific problem crucially depends on appropriately choosing trial vector generation strategies and their associated control parameter values namely the step size F, crossover probability CR, number of population NP and generations G [17].

In view of the above, a Differential Evolution (DE) optimized fuzzy PID controller is proposed for Load Frequency Control (LFC) of multi-area multi-units thermal–thermal power system with the consideration of reheat turbine, Generation Rate Constraint (GRC) and time delay. The superiority of the proposed approach is shown by comparing the results with GA for the same power system. Further, TCSC is employed in series with the tie-line in coordination with SMES to improve the dynamic performance of the power system. Finally, sensitivity analysis is carried out by varying the loading condition and system parameters.

2. Materials and methods

2.1. System under study

The system under investigation consists of two area interconnected thermal power system as shown in Fig. 1. Area 1 comprises two reheat thermal power units. Area 2 comprises two non-reheat thermal units. In Fig. 1, B_1 and B_2 are the frequency bias parameters; ACE_1 and ACE_2 are area control errors; R_1, R_2 and R_3, R_4 are the governor speed regulation parameters in pu Hz for area 1 and area 2 respectively; T_{G1}, T_{G2} and T_{G3}, T_{G4} are the speed governor time constants in sec for area 1 and area 2 respectively; T_{T1}, T_{T2} and T_{T3}, T_{T4} are the turbine time constant in sec for area 1 and area 2 respectively; ΔP_{D1} and ΔP_{D2} are the load demand changes; ΔP_{Tie} is the incremental change in tie line power (p.u); K_{Ps1} and K_{Ps2} are the power system gains; T_{Ps1} and T_{Ps2} are the power system time constant in sec; T_{12} is the synchronizing coefficient and ΔF_1 and ΔF_2 are the system frequency deviations in Hz. To get an accurate insight into the AGC problem, it is essential to include the important inherent requirement and the basic physical constraints and include them model. The important constraints that affect the power system performance are Generation Rate Constraint (GRC), and Time delay. In view of the above, the effect of GRC and Time delay are included to a power system model. Time delays can degrade a system's performance and even cause system instability. In a power system having steam plants, power generation can change only at a specified maximum rate. In thermal power plants, power generation can change only at a specified maximum/minimum rate known as Generation Rate Constraint (GRC). In the present study, a GRC of 3%/min for reheat and 10%/ min for non-reheat thermal units are considered [18,19]. Also in the present study, a time delay of 50 ms is considered [20]. The relevant parameters are given in Appendix A.

2.2. Control structure and objective function

To control the frequency, fuzzy PID controllers are provided in each area. The structure of fuzzy PID controller is shown in Fig. 2 [21,22].

The error inputs to the controllers are the respective area control errors (ACE) given by:

$$e_1(t) = ACE_1 = B_1\Delta F_1 + \Delta P_{Tie} \quad (1)$$

$$e_2(t) = ACE_2 = B_2\Delta F_2 - \Delta P_{Tie} \quad (2)$$

Fuzzy controller uses error (e) and derivative of error ($\dot{e}$) as input signals. The outputs of the fuzzy controllers u_1 and u_2 are the control inputs of the power system i.e. the reference power settings ΔP_{ref1} and ΔP_{ref2}. The input scaling factors are the tuneable parameters K_1 and K_2. The proportional, integral and derivative gains of fuzzy controller are represented by K_P, K_I and K_D respectively. Triangular membership functions are used with five fuzzy linguistic variables such as NB (negative big), NS (negative small), Z (zero), PS (positive small) and PB (positive big) for both the inputs and the output. Membership functions for error, error derivative and FLC out-

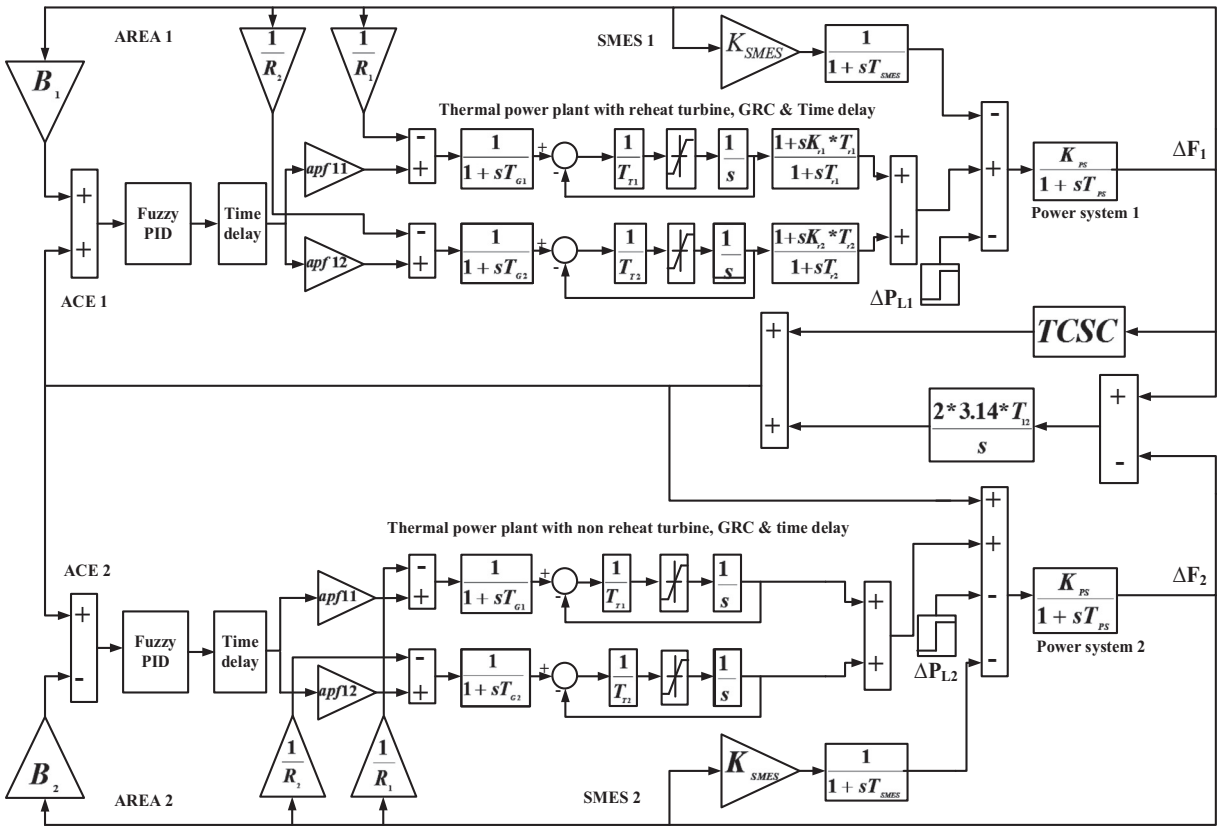

Figure 1 MATLAB/SIMULINK model of multi-area multi-units thermal system.

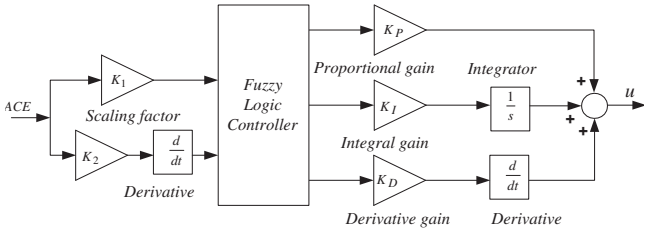

Figure 2 Structure of proposed fuzzy PID controller.

put are shown in Fig. 3. Mamdani fuzzy interface engine is selected for this work. The FLC output is determined by using center of gravity method of defuzzification. The two-dimensional rule base for error, error derivative and FLC output is shown in Table 1.

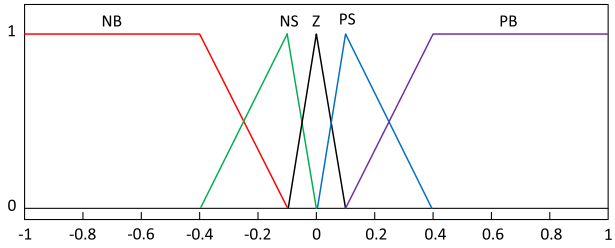

Figure 3 Membership functions for error, error derivative and FLC output.

Table 1 Rule base for error, derivative of error and FLC output.

e	$\dot{e}$				
	NB	NS	Z	PS	PB
NB	NB	NB	NS	NS	Z
NS	NB	NS	NS	Z	PS
Z	NS	NS	Z	PS	PS
PS	NS	Z	PS	PS	PB
PB	Z	PS	PS	PB	PB

In the design of modern heuristic optimization technique based controller, the objective function is first defined based on the desired specifications and constraints. Typical output specifications in the time domain are peak overshooting, rise time, settling time, and steady-state error. It has been reported in the literature that Integral of Time multiplied Absolute Error (ITAE) gives a better performance compared to other integral based performance criteria [23]. Therefore in this paper ITAE is used as objective function to optimize the scaling factors and proportional, integral and derivative gains of fuzzy PID controller. Expression for the ITAE objective function is depicted in Eq. (3).

$$J = ITAE = \int_0^{t_{sim}} (|\Delta F_1| + |\Delta F_2| + |\Delta P_{Tie}|) \cdot t \cdot dt \tag{3}$$

In the above equation, ΔF_1 and ΔF_2 are the system frequency deviations; ΔP_{Tie} is the incremental change in tie line power; t_{sim} is the time range of simulation.

2.3. Modeling of TCSC in AGC

It is well known that the reactance adjusting of Thyristor Controlled Series Compensator (TCSC) is a complex dynamic process. Effective design and accurate evaluation of the TCSC control strategy depends on the simulation accuracy of this process. Basically a TCSC consists of three components: capacitor banks, bypass inductor and bidirectional thyristors. The firing angles of the thyristors are controlled to adjust the TCSC reactance in accordance with a system control algorithm, normally in response to some system parameter variations. According to the variation in the thyristor firing angle, this process can be modeled as a fast switch between corresponding reactance offered to the power system. Both capacitive and inductive reactance compensation are possible by proper selection of capacitor and inductor values of the TCSC device. TCSC is considered as a variable reactance, the value of which is adjusted automatically to constrain the power flow across the branch to a specified value. The variable reactance X_{TCSC} represents the net equivalent reactance of the TCSC, when operating in either the inductive or the capacitive mode [14]. Fig. 4 shows the schematic diagram of a two area interconnected thermal-thermal power system with TCSC connected in series with the tie-line. For analysis, it is assumed that TCSC is connected near to the area 1. Resistance of the tie-line is neglected, since the effect on the dynamic performance is negligible. Further, the reactance to resistance ratio in a practically interconnected power system is quite high. The incremental tie-line power flow without TCSC is given by (4).

$$\Delta P_{Tie12}(s) = \frac{2\pi T_{12}^0}{s}[\Delta F_1(s) - \Delta F_2(s)] \tag{4}$$

In the above equation, ΔF_1 and ΔF_2 are the system frequency deviations; T_{12}^0 is the synchronizing coefficient without TCSC. The line current flow from area-1 to area-2 can be written as, when TCSC is connected in series with the tie-line

$$I_{12} = \frac{|V_1|\angle(\delta_1) - |V_2|\angle(\delta_2)}{j(X_{12} - X_{TCSC})} \tag{5}$$

where X_{12} and X_{TCSC} are the tie-line and TCSC reactance respectively.

It is clear from Fig. 4 that, the complex tie-line power as

$$P_{Tie12} - jQ_{Tie12} = V_1^* I_{12} = |V_1|\angle(-\delta_1)\left[\frac{|V_1|\angle(\delta_1) - |V_2|\angle(\delta_2)}{j(X_{12} - X_{TCSC})}\right] \tag{6}$$

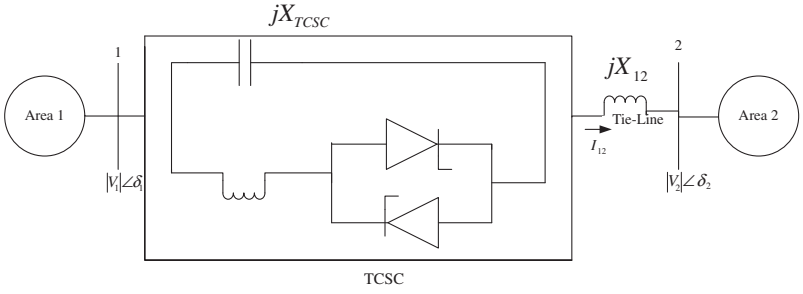

Figure 4 Two-area interconnected power system with TCSC.

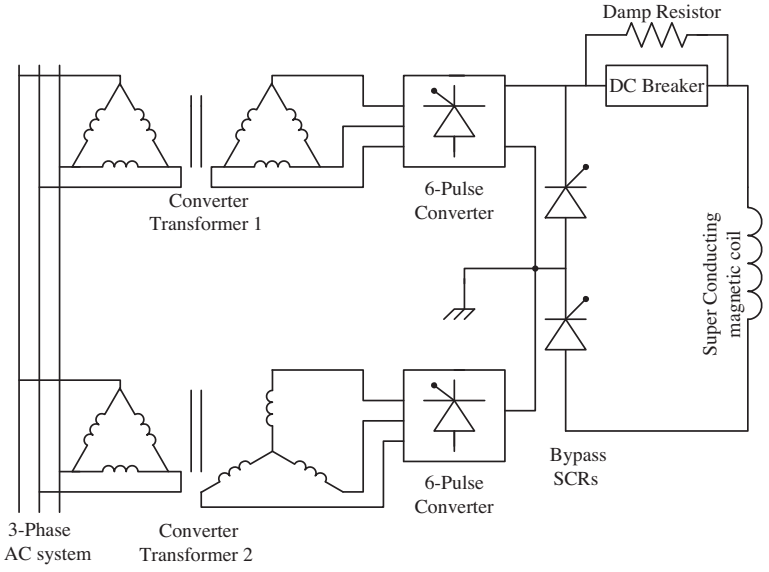

Figure 5 SMES circuit diagram.

Solving the above equation, the real part,

$$P_{Tie12} = \frac{|V_1||V_2|}{(X_{12} - X_{TCSC})} \sin(\delta_1 - \delta_2) \tag{7}$$

The tie-line power flow can be represented in terms of % compensation (k_c) as

$$P_{Tie12} = \frac{|V_1||V_2|}{X_{12}(1 - k_C)} \sin(\delta_1 - \delta_2) \tag{8}$$

where $k_c = \frac{X_{TCSC}}{X_{12}}$, percentage of compensation offered by the TCSC

In order to obtain the linear incremental model, Eq. (8) can be rewritten as

$$\Delta P_{Tie12} = \frac{|V_1||V_2|}{X_{12}(1 - k_C^0)^2} \sin(\delta_1^0 - \delta_2^0)\Delta k_C + \frac{|V_1||V_2|}{X_{12}(1 - k_C^0)} \times \cos(\delta_1^0 - \delta_2^0)(\Delta\delta_1 - \Delta\delta_2) \tag{9}$$

If $J_{12}^0 = \frac{|V_1||V_2|}{X_{12}} \sin(\delta_1^0 - \delta_2^0)$ and $T_{12}^0 = \frac{|V_1||V_2|}{X_{12}} \cos(\delta_1^0 - \delta_2^0)$, then Eq. (9) is expressed as

$$\Delta P_{Tie12} = \frac{J_{12}^0}{(1 - k_C^0)^2}\Delta k_C + \frac{T_{12}^0}{(1 - k_C^0)}(\Delta\delta_1 - \Delta\delta_2) \tag{10}$$

Since $\Delta\delta_1 = 2\pi \int \Delta F_1 dt$ and $\Delta\delta_2 = 2\pi \int \Delta F_2 dt$

Taking Laplace transforms of Eq. (10) and expressed as given by (11)

$$\Delta P_{Tie12}(s) = \frac{J_{12}^0}{(1 - k_C^0)^2}\Delta k_C(s) + \frac{2\pi T_{12}^0}{s(1 - k_C^0)}[\Delta F_1(s) - \Delta F_2(s)] \tag{11}$$

From Eq. (11), the tie-line power flow can be regulated by controlling $\Delta k_c(s)$. If the control input signal to TCSC damping controller is assumed to be ΔError(s) and the transfer function of the signal conditioning circuit is $k_c = \frac{K_{TCSC}}{1 + sT_{TCSC}}$, The expression is given (12)

$$\Delta k_C(s) = \frac{K_{TCSC}}{1 + sT_{TCSC}} \Delta\text{Error}(s) \tag{12}$$

where K_{TCSC} and T_{TCSC} is the gain and time constant of the TCSC controller respectively. As TCSC is kept near to area-1, frequency deviation ΔF_1 may be suitably used as the control signal ΔError(s), to the TCSC unit to control the percentage incremental change in the system compensation level. Therefore,

$$\Delta k_C(s) = \frac{K_{TCSC}}{1 + sT_{TCSC}} \Delta F_1(s) \tag{13}$$

$$\Delta P_{Tie12} = \frac{2\pi T_{12}^0}{s(1 - k_C^0)}[\Delta F_1(s) - \Delta F_2(s)] + \left[\frac{J_{12}^0}{(1 - k_C^0)^2}\right] \frac{K_{TCSC}}{1 + sT_{TCSC}} \Delta F_1(s) \tag{14}$$

2.4. Modeling of SMES in AGC

Superconducting Magnetic Energy Storage (SMES) is a device which can store the electrical power from the grid in the magnetic field of a coil. The magnetic field of coil is made of superconducting wire with near-zero loss of energy. SMESs can store and refurbish huge values of energy almost instantaneously. Therefore the power system can discharge high levels of power within a fraction of a cycle to avoid a rapid loss in the line power. The SMES is consisting of inductor-converter unit, dc superconducting inductor, AC/ DC converter and a step down transformer [24]. The stability of a SMES unit is superior to other power storage devices, because all parts of a SMES unit are static. Fig. 5 shows the schematic diagram of SMES unit in the power system [13]. During normal operation of the grid, the superconducting coil will be charged to a set value (normally less than the maximum charge) from the utility grid. After charged, the superconducting coil conducts current, which supports an electromagnetic field, with virtually no losses. The coil is kept at very low temperature by immersion in a bath of liquid helium.

In the present work two SMES units are established in area1 and area2 in order to stabilize frequency oscillations as shown in Fig. 1. The input signal of the SMES controller is p.u. frequency deviation (ΔF) and the output is the change in control vector [ΔP_{SMES}]. The controller gains K_{SMES} and the time constant T_{SMES} values are 0.12 and 0.03 s respectively [24].

3. Over view of differential evolution

Differential Evolution (DE) algorithm is a search heuristic algorithm introduced by Storn and Price [15]. It is a simple, efficient, reliable algorithm with easy coding. The main advantage of DE over Genetic Algorithm (GA) is that GA uses crossover operator for evolution while DE relies on mutation operation. The mutation operation in DE is based on the difference in randomly sampled pairs of solutions in the population. An optimization task consisting of D variables can be represented by a D-dimensional vector. A population of N_P solution vectors is randomly initialized within the parameter bounds at the beginning. The population is modified by applying mutation, crossover and selection operators. DE algorithm uses two generations; old generation and new generation of the same population size. Individuals of the current population become target vectors for the next generation. The mutation operation produces a mutant vector for each target vector, by adding the weighted difference between two randomly chosen vectors to a third vector. A trial vector is generated by the crossover operation by mixing the parameters of the mutant vector with those of the target vector. The trial vector substitutes the target vector in the next generation if it obtains a better fitness value than the target vector. The evolutionary operators are described below [25,26]:

3.1. Initialization of parameter

DE begins with a randomly initiated population of size N_P *of* D dimensional real-valued parameter vectors. Each parameter j lies within a range and the initial population should spread over this range as much as possible by uniformly randomizing individuals within the search space constrained by the prescribed lower bound X_j^L and upper bound X_j^U.

3.2. Mutation operation

For the mutation operation, a parent vector from the current generation is selected (known as target vector), a mutant vec-

tor is obtained by the differential mutation operation (known as donor vector) and finally an offspring is produced by combining the donor with the target vector (known as trial vector). Mathematically it can be expressed as:

$$V_{i,G+1} = X_{r1,G} + F.(X_{r2,G} - X_{r3,G}) \quad (15)$$

where $X_{i,G}$ is the given parameter vector, $X_{r1,G}$ $X_{r2,G}$ $X_{r3,G}$ are randomly selected vector with distinct indices i, $r1$, $r2$ and $r3$, $V_{i,G+1}$ is the donor vector and F is a constant from $(0, 2)$

3.3. Crossover operation

After generating the donor vector through mutation the crossover operation is employed to enhance the potential diversity of the population. For crossover operation three parents are selected and the child is obtained by means of perturbation of one of them. In crossover operation a trial vector $U_{i,G+1}$ is obtained from target vector $(X_{i,G})$ and donor vector $(V_{i,G})$. The donor vector enters the trial vector with probability CR given by:

$$U_{j,i,G+1} = \begin{cases} V_{j,i,G+1} & \text{if } rand_{j,i} \leqslant CR \quad or \quad j = I_{rand} \\ X_{j,i,G+1} & \text{if } rand_{j,i} > CR \quad or \quad j \neq I_{rand} \end{cases}$$

With $rand_{j,i} \sim U(0, 1)$, I_{rand} is a random integer from $(1, 2, \ldots, D)$ where D is the solution's dimension i.e. number of control variables. I_{rand} ensures that $V_{i,G+1} \neq X_{i,G}$.

3.4. Selection operation

To keep the population size constant over subsequent generations, selection operation is performed. In this operation the target vector $X_{i,G}$ is compared with the trial vector $V_{i,G+1}$ and the one with the better fitness value is admitted to the next generation. The selection operation in DE can be represented by:

$$X_{i,G+1} = \begin{cases} U_{i,G+1} & \text{if } f(U_{i,G+1}) < f(X_{i,G}) \\ X_{i,G} & \text{otherwise.} \end{cases}$$

where $i \in [1, NP]$.

4. Results and discussions

4.1. Implementation of DE

The effectiveness, efficiency, and robustness of the DE algorithm are sensitive to the settings of the control parameters. The control parameters in DE are step size function also called scaling factor (F), crossover probability (CR), the number of population (N_P), initialization, termination and evaluation function. F controls the amount of perturbation in the mutation process and generally lies in the range $(0, 1)$. Crossover probability (CR) constants are generally chosen from the interval $(0.5, 1)$. Several strategies can be employed in DE optimization algorithm. The strategy in a DE algorithm is denoted by DE/x/y/z, where x represents the mutant vectors, y represents the number of difference vectors used in the mutation process and z represents the crossover scheme used in the crossover operation. The suggested choice of control parameters is [25] population size of N_P = 50 (N_P = 5D where D = dimensionality of the problem), step size F = 0.8 and crossover probability of CR = 0.8 and these values are selected in the present paper. The strategy employed is as follows: DE/best/1/exp. Optimization is terminated by the pre-specified number of generations which is set to 100. The flow chart of the DE algorithm employed in the present study is given in Fig. 6. The model of the system under study shown in Fig. 1 is developed in MATLAB/SIMULINK environment and DE program is written (in .mfile). Initially, fuzzy PID controllers without TCSC and SMES units are considered for each area. Scaling factors and PID controller gains are chosen in the range [0 −2] and [−2 2] respectively. The developed model is simulated in a separate program (by .mfile using initial population/controller parameters) considering a 1% step load change in area 1. The objective function (ITAE) value for each individual is calculated in the SIMULINK model file and transferred to .mfile through workspace. These objective function values are used to assess the populations. The population is then modified by applying mutation, crossover and selection operators in the main DE program as given in Flow chart (Fig. 6). Simulations were conducted on an Intel, core i-3core cpu, of 2.4 GHz and 4 GB RAM computer in the MATLAB 7.10.0.499 (R2010a) environment. The optimization was repeated 50 times and the best final solution among the 50 runs is chosen as proposed controller parameters. The best final solutions obtained in the 50 runs are shown in Table 2.

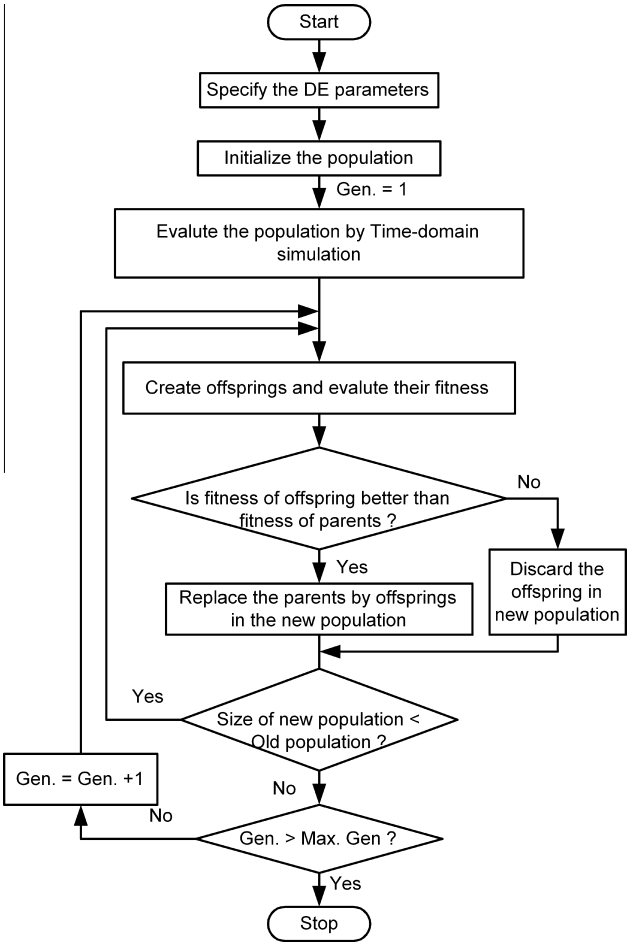

Figure 6 Flow chart of proposed DE optimization approach.

4.2. Analysis of results

The objective function (ITAE) value given by Eq. (3) is determined by simulating the developed model by applying a 1% step increase in load in area 1. The corresponding performance index in terms of ITAE value, settling times (2%) and peak overshoots in frequency and tie line power deviations is shown in Table 3. For comparison, the corresponding values of GA optimized fuzzy PID controllers are also shown in Table 3. For the implementation of GA, normal geometric selection, arithmetic crossover and non-uniform mutation are employed in the present study. A population size of 50 and maximum generation of 100 is employed in the present paper. A detailed description about GA parameters employed in the present paper can be found in reference [9]. It should be noted here that, GA values correspond to same power system, controller

Table 2 Tuned fuzzy PID controller parameters.

Optimum controller gains	Genetic Algorithm (GA)	Differential Evolution (DE)		
	Without TCSC and SMES	Without TCSC and SMES	With TCSC	With TCSC and SMES
K_1	1.5553	1.8589	0.1943	0.1132
K_2	1.7920	1.9092	1.5638	1.6820
K_{P1}	−0.0805	0.5481	1.6720	1.5621
K_{I1}	1.3460	1.9461	1.7881	1.5075
K_{D1}	1.3483	0.5170	−0.6707	−0.3560
K_3	1.9128	0.3338	0.5414	0.1932
K_4	0.2626	0.3607	0.2572	0.3662
K_{P2}	0.2813	− 0.2837	−0.9896	−1.7376
K_{I2}	1.1323	−0.8919	−0.2052	1.3894
K_{D2}	−0.0970	1.3173	0.9608	−1.0557

Table 3 Comparative performance of error and settling time.

Parameters	ITAE	Settling time (2% band), T_s (s)			Peak over shoot ($\times 10^{-3}$)		
		ΔF_1	ΔF_2	ΔP_{Tie}	ΔF_1	ΔF_2	ΔP_{Tie}
GA	2.1429	37.05	34.85	34.06	6.413	1.568	0.839
DE	1.2250	33.26	35.03	30.43	3.974	1.528	0.756
DE: with TCSC	0.8178	21.84	22.25	26.25	3.768	8.010	0.762
DE: both TCSC and SMES	**0.6672**	**21.13**	**21.57**	**16.85**	**2.5113**	**5.440**	**0.290**

The bold values are indicates the best results.

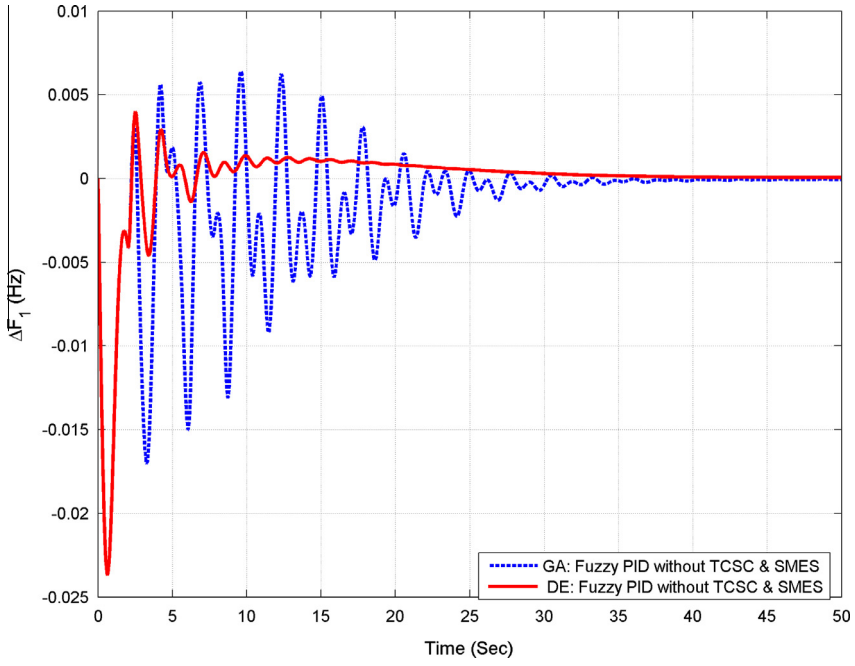

Figure 7 Change in frequency of area-1 for 1% load change in area-1 without TCSC and SMES units.

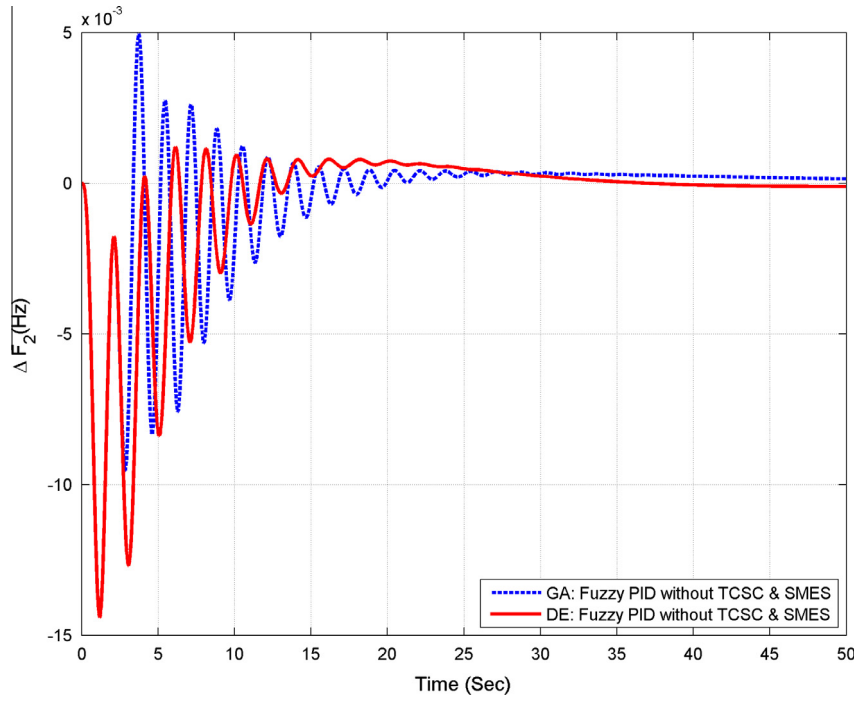

Figure 8 Change in frequency of area-2 for 1% load change in area-1 without TCSC and SMES units.

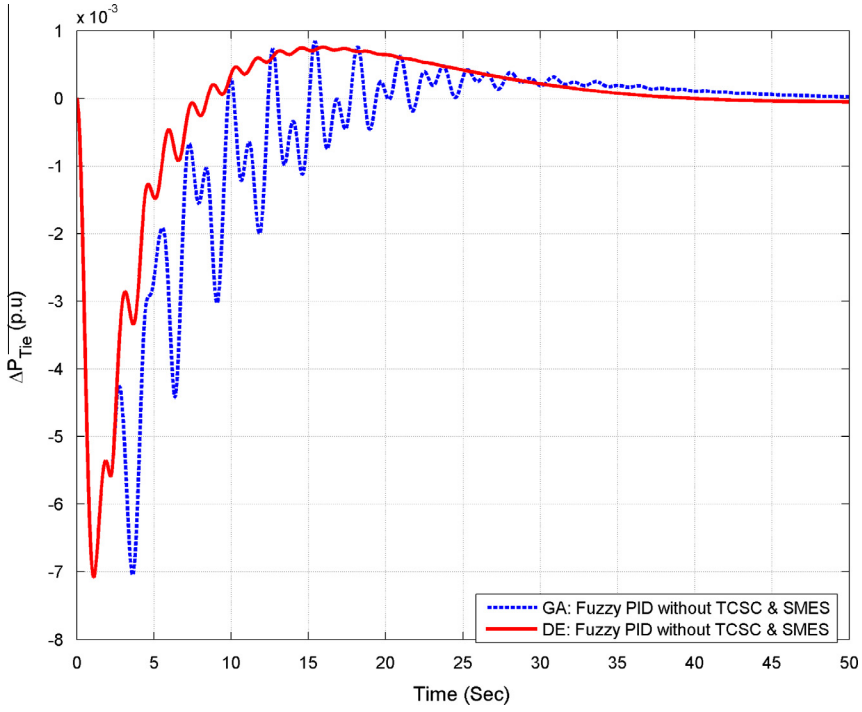

Figure 9 Change in tie line power for 1% load change in area-1 without TCSC and SMES units.

structure (fuzzy PID) and objective function employed (ITAE) for proper comparison of techniques. It is evident from Table 3 that DE outperform GA as minimum ITAE value is obtained with DE (ITAE = 1.2250) compared to GA (ITAE = 2.1429). The dynamic performance of the system is shown in Figs. 7–9 for 1% step increase in load in area 1. It is clear from Figs. 7–9 that better dynamic performance is obtained by DE optimized fuzzy PID controller compared to GA optimized fuzzy PID controller. Hence it can be concluded that DE outperform GA technique.

In the next step, the TCSC is incorporated separately in the tie-line to analysis its effect on the power system performance. Subsequently SMES units are installed in both areas and coordinated with TCSC to study their effect on system perfor-

mance. The results of fuzzy PID controller with TCSC employing differential evolution algorithm over 50 independent runs are shown in Table 2. It is clear from Table 3 that by employing the TCSC along with fuzzy PID controller, the objective function (ITAE) value is decreased to 0.8178 (i.e. 33.24% improvement). In addition better results are observed in terms of settling time and peak overshoot values with the TCSC fuzzy PID compared to without TCSC. It is also seen that with coordinated application of TCSC and SMES units, the ITAE value is further reduced to **0.6672**. It can be seen from Table 3 that with TCSC and SMES, the settling times of ΔF_1, ΔF_2 and ΔP_{Tie} are improved compared to others for the same investigated system with similar objective function (ITAE).

To study the dynamic performance of the system a step increase in demand of 1% is applied at $t = 0$ s in area-1 and the system dynamic responses are shown in Figs. 10–12. Crit-

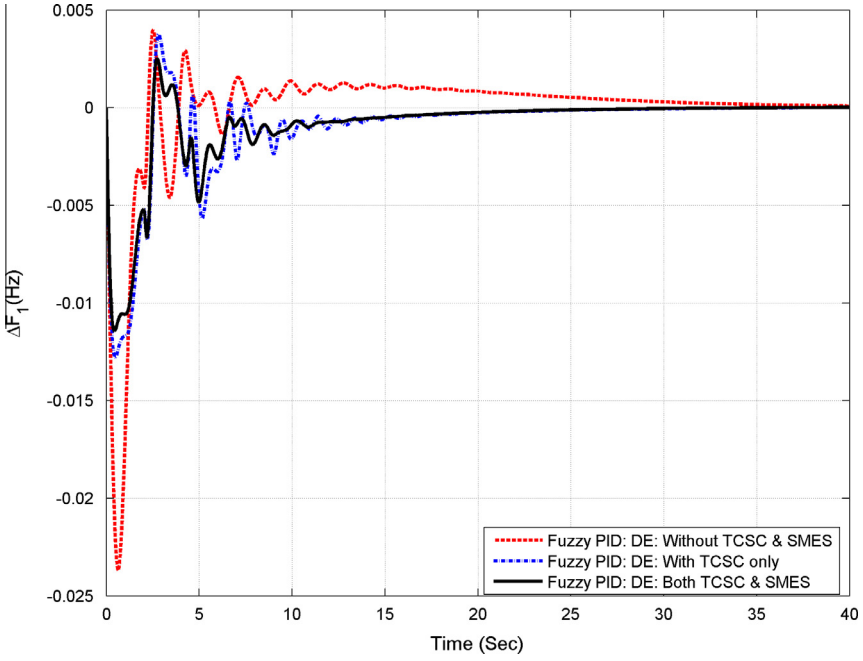

Figure 10 Change in frequency of area-1 for 1% load change in area-1.

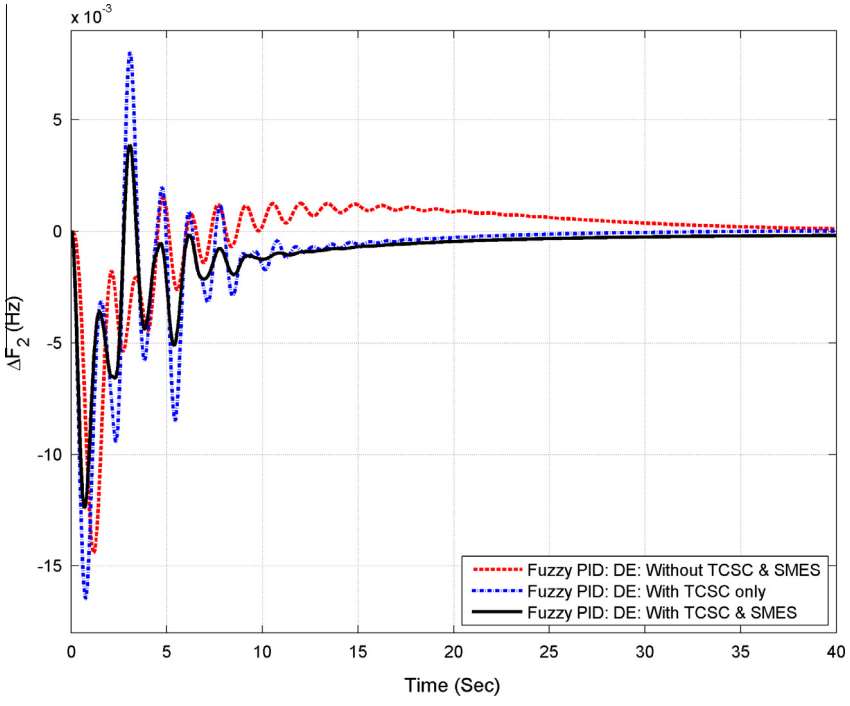

Figure 11 Change in frequency of area-2 for 1% load change in area-1.

ical analysis of the dynamic responses clearly reveals that significant system performance improvement in terms of minimum undershoot and overshoot in frequency oscillations as well as tie-line power exchange is observed with coordinated application of TCSC and SMES units.

4.3. Sensitivity analysis

Sensitivity analysis is carried out to study the robustness the system to wide changes in the operating conditions and system parameters [5,27,28]. In this section robustness of the power system is checked by varying the loading conditions and system parameters from their nominal values (given in Appendix A) in the range of +25% to −25% without changing the optimum values of fuzzy PID controller gains. The change in operating load condition affects the power system parameters K_P and T_P. The power system parameters are calculated for different loading conditions as given in Appendix A. The system with TCSC and SMES units are considered in all the cases due to their superior performance. The various performance indexes (settling time, peak overshoot and ITAE) under normal and parameter variation cases for the system are given in Table 4. It can be observed from Table 4 that settling time, peak overshoot and ITAE values vary within acceptable ranges and are nearby equal to the respective values obtained with nominal system parameter. It is also evident from Tables 5 and 6 that the eigenvalues lie in the left half of s-plane for all the cases thus maintain the stability. Hence, it can be con-

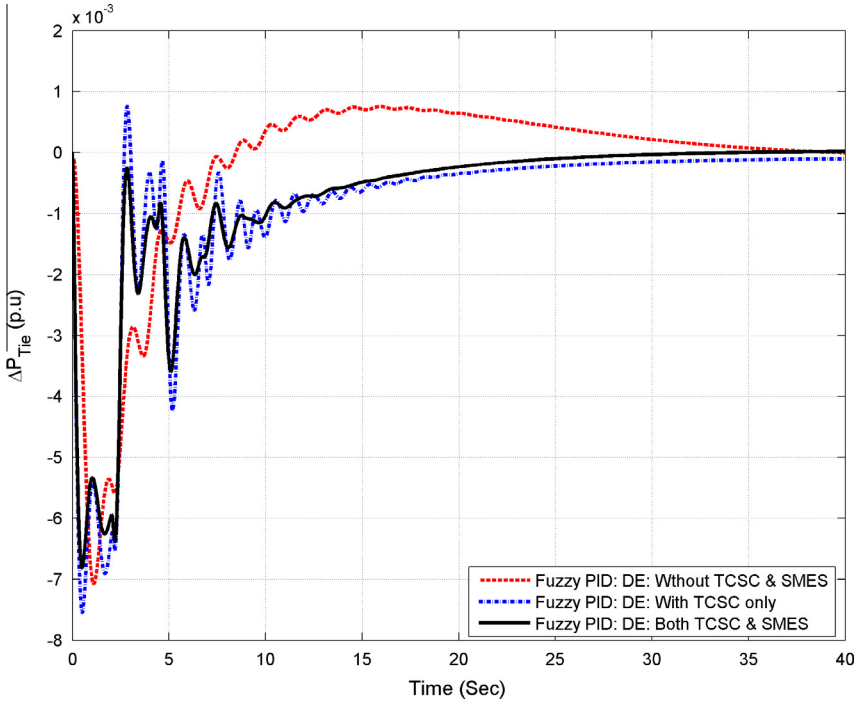

Figure 12 Tie-line power deviation for 1% load change in area-1.

Table 4 Sensitivity analysis.

Parameter variation	% Change	Performance index with TCSC and SMES						ITAE
		Settling time, T_s (s)			Peak over shoot $\times 10^{-3}$			
		ΔF_1	ΔF_2	ΔP_{Tie}	ΔF_1	ΔF_2	ΔP_{Tie}	
Nominal	**0**	**21.13**	**21.57**	**16.85**	**2.5113**	**5.440**	**0.290**	**0.6672**
Loading condition	+25	21.83	22.22	17.15	2.489	5.364	0.266	0.6650
	−25	20.47	20.88	16.40	2.533	5.517	0.313	0.6825
T_G	+25	23.03	23.45	17.59	2.835	5.895	0.488	0.7144
	−25	19.31	19.76	15.87	2.147	4.946	0.171	0.7351
T_t	+25	19.44	19.87	15.94	2.564	5.480	0.298	0.7203
	−25	23.29	23.68	17.68	2.395	5.291	0.233	0.7256
B	+25	20.63	21.10	17.37	2.493	5.530	0.299	0.6492
	−25	21.65	22.04	16.14	2.531	5.354	0.280	0.6912
R	+25	21.48	21.89	17.11	2.494	5.485	0.194	0.7069
	−25	20.68	21.13	16.32	2.514	5.362	0.422	0.6103

The bold values are indicates the best results.

cluded that the proposed controllers are robust and perform satisfactorily when system parameters changes in the range ±25%. The dynamic performance of the system with the varied conditions of loading, T_G, T_T, B and R is shown in Figs. 13–19. It can be observed from Figs. 13–19 that the effect of the variation in loading condition and system parameters on the system performance is negligible. Hence the optimum values of controller parameters obtained at the nominal loading with nominal parameters, need not be reset for wide changes in the system loading or system parameters.

5. Conclusion

In this paper, a Differential Evolution (DE) algorithm optimized fuzzy PID controller has been proposed for Automatic Generation Control (AGC) of multi-area multi-units power systems. Initially a multi-area multi-units power system with the considerations of physical constraints such as GRC and time delays is considered and the superiority of DE over GA is demonstrated. A linear incremental model for a TCSC has also been developed which is suitable for AGC applications. Further, TCSC and SMES units are added in the system model in order to improve the system performance. It is observed that when the TCSC unit is placed with the tie-line, dynamic performance of system is improved. Then the impact of SMES units in the AGC along with TCSC is studied. From the simulation results, it is observed that significant improvements of dynamic responses are obtained with coordinated application of TCSC and SMES units. Finally, sensitivity analysis is carried out to show the robustness of the controller by varying the loading conditions and system parameters in the range of +25% to −25% from their nominal values. For systems under study, it is revealed that the parameters of the proposed DE optimized fuzzy PID controllers need not be reset even if the system is subjected to wide variation in loading conditions and system parameters.

Table 5 System eigen values under parameter variation in loading, T_G and T_T with TCSC and SMES units.

Loading condition		T_G		T_T	
+25%	−25%	+25%	−25%	+25%	−25%
−48.2086	−48.2096	−48.2093	−48.2086	−48.2093	−48.2088
−31.9578	−31.9592	−31.9596	−31.9561	−31.9593	−31.9572
−33.0234	−33.0237	−33.0236	−33.0236	−33.0236	−33.0236
−13.4364	−13.4354	−13.4629	−16.9560	−13.4497	−13.4189 ± 0.0790i
−13.2648	−13.2628	−12.9373	−13.4694	−13.1737	−1.4553 ± 4.7764i
−1.3825 ± 4.7594i	−1.3708 ± 4.7614i	−10.3946	−12.8478	−1.3341 ± 4.7430i	−1.2922 ± 3.0029i
−1.3825 ± 2.8736i	−1.2456 ± 2.8684i	−1.3570 ± 4.7719i	−1.3943 ± 4.7438i	−1.2419 ± 2.7746i	−2.7612
−1.3360	−1.3376	−1.2261 ± 2.8569i	−1.2809 ± 2.8822i	−2.1386	−1.3774
−0.1269	−0.1271	−1.3324	−1.3411	−1.2845	−0.1269
−0.0107	−0.0107	−0.1270	−0.1270	−0.1271	−0.0107
−0.0047	−0.0047	−0.0107	−0.0107	−0.0107	−0.0047
−0.1000	−0.1000	−0.0047	−0.0047	−0.0047	−2.3810
−12.4999	−12.5000	−12.5000	−12.5000	−2.3810	−0.1000
−12.5000	−12.5000	−0.1000	−0.1000	−0.1000	−12.5000
−2.3809	−2.3810	−2.3810	−2.3810	−12.5000	−12.5000
−2.3809	−2.3810	−2.3810	−2.3810	−12.5000	

Table 6 System eigen values under parameter variation in B and R with TCSC and SMES units.

B		R	
+25%	−25%	+25%	−25%
−48.2091	−48.2091	−48.2093	−48.2088
−31.9620	−31.9556	−31.9592	−31.9574
−32.9426	−33.1037	−33.0236	−33.0236
−13.4426	−13.4293	−13.4482	−13.4023 ± 0.0620i
−13.2631	−13.2646	−13.1869	−1.4277 ± 4.8201i
−1.3964 ± 4.7793i	−1.3573 ± 4.7410i	−1.3443 ± 4.7293i	−1.1697 ± 2.9829i
−1.2685 ± 2.8656i	−1.2363 ± 2.8767i	−1.3022 ± 2.7924i	−1.2936
−1.3362	−1.3374	−1.3679	−0.1305
−0.1270	−0.1270	−0.1247	−0.0109
−0.0051	−0.0104	−0.0106	−0.0043
−0.0111	−0.0043	−0.0050	−0.1000
−0.1000	−0.1000	−0.1000	−12.5000
−12.5000	−12.5000	−12.5000	−12.5000
−12.5000	−12.5000	−12.5000	−2.3810
−2.3810	−2.3810	−2.3810	−2.3810
−2.3810	−2.3810	−2.3810	

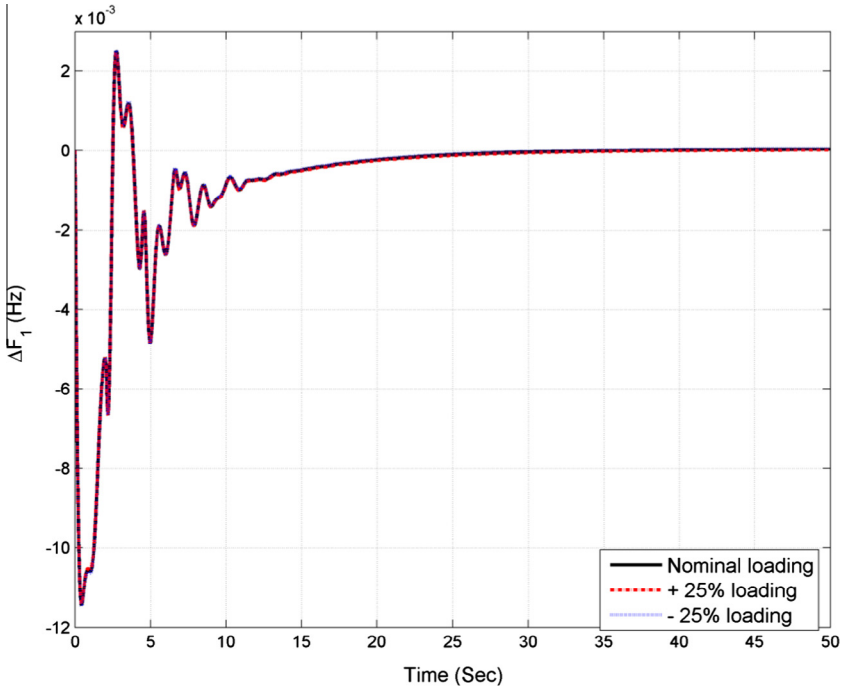

Figure 13 Change in frequency of area-1 for 1% load change in area-1 with variation in loading.

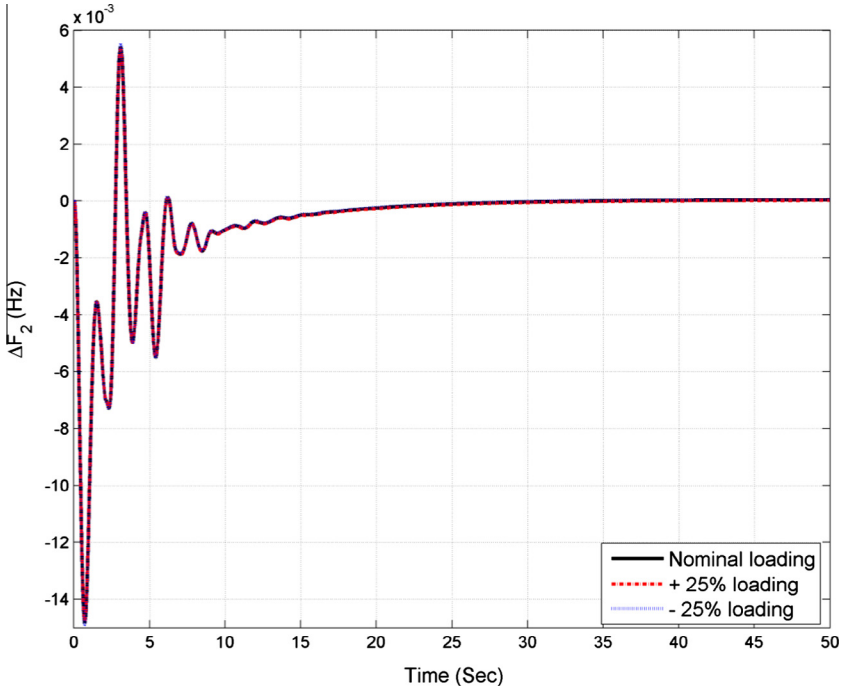

Figure 14 Change in frequency of area-2 for 1% load change in area-1 with variation in loading.

Appendix A

Nominal parameters of the system investigated are:

(i) **Multi-area multi-units system**

$B_1, B_2 = 0.42249$ p.u. MW/Hz; $R_1 = R_2 = R_3 = R_4 = 2.4$ Hz/p.u.; $T_{G1} = T_{G2} = T_{G3} = T_{G4} = 0.08$ s; $T_{T1} = T_{T2} = T_{T3} = T_{T4} = 0.3$ s; $K_P = 120$ Hz/p.u.; TP $= 20$ s;$K_{R1} = K_{R2} = 10$; $T_{R1} = T_{R2} = 10$ s

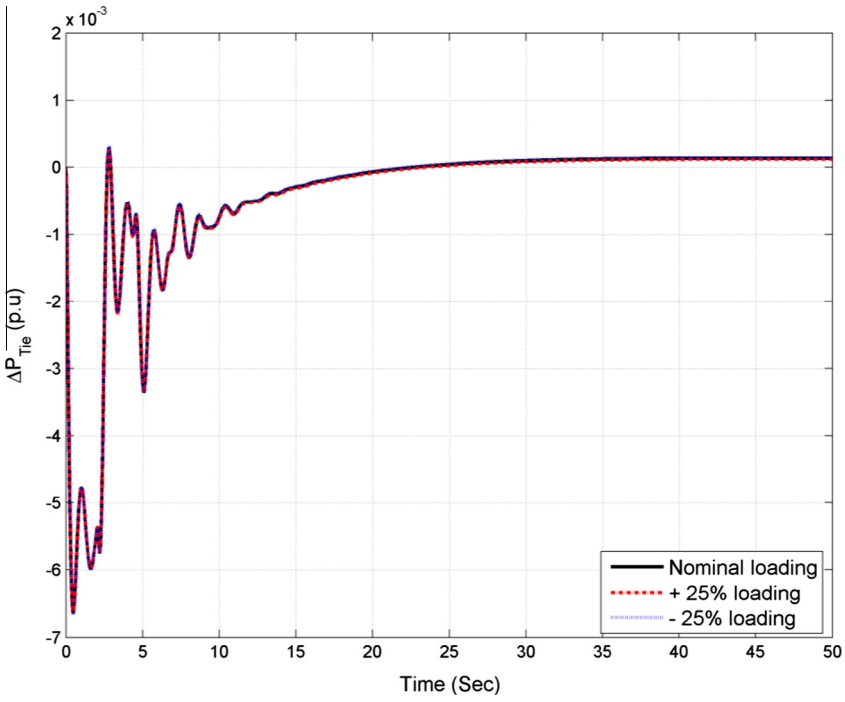

Figure 15 Tie-line power deviation for 1% load change in area-1 with variation in loading.

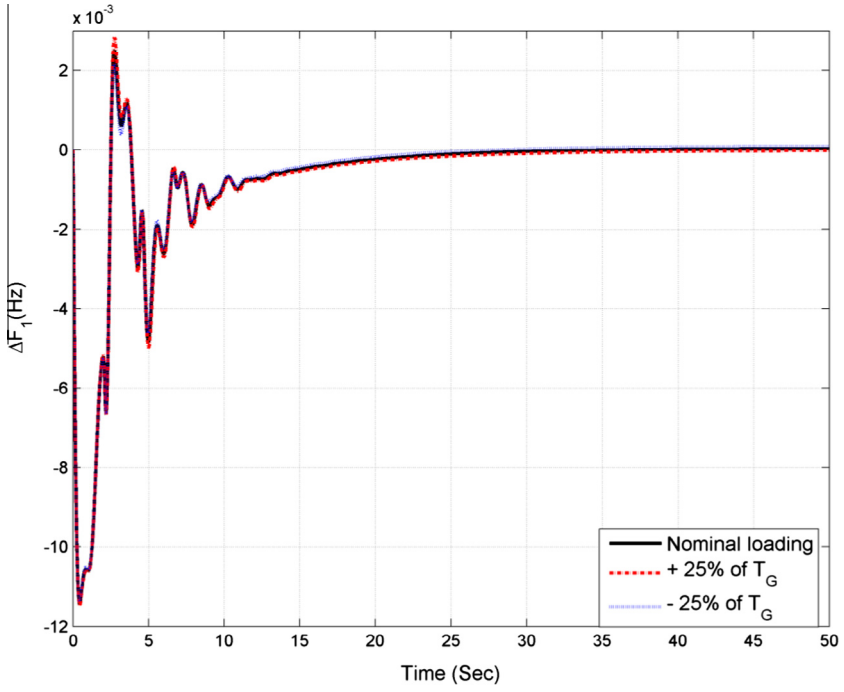

Figure 16 Change in frequency of area-1 for 1% load change in area-1 with variation in T_G.

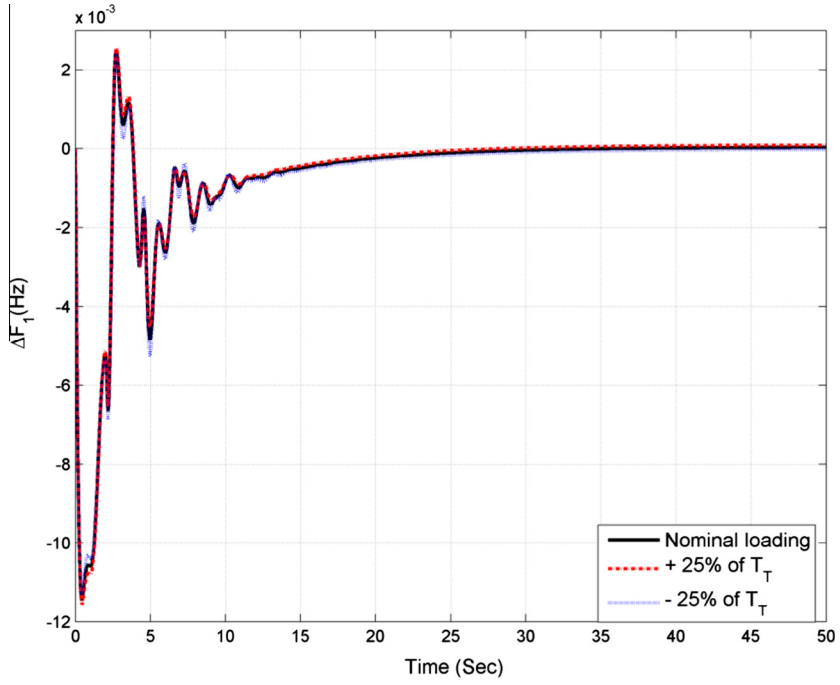

Figure 17 Change in frequency of area-1 for 1% load change in area-1 with variation in T_T.

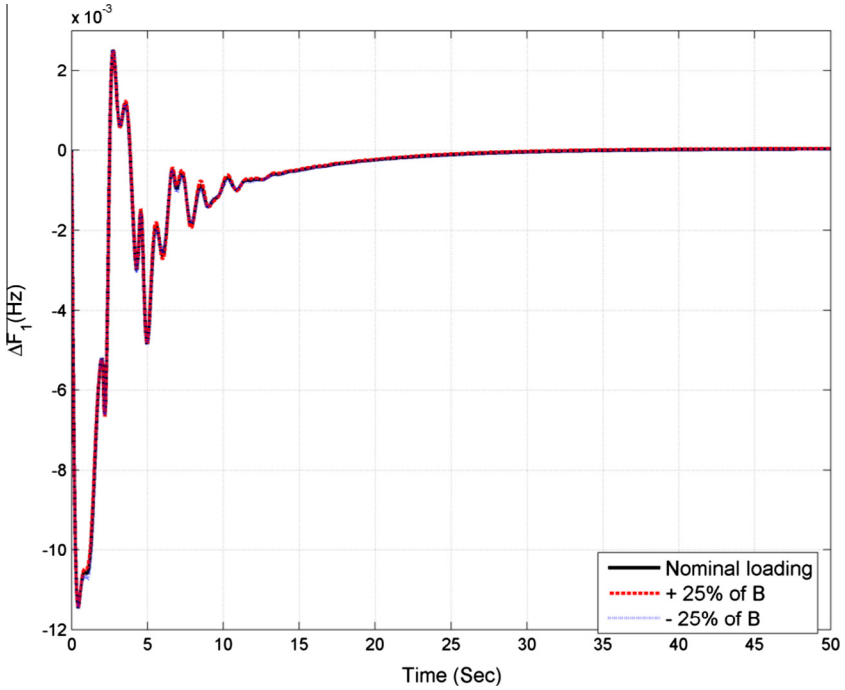

Figure 18 Change in frequency of area-1 for 1% load change in area-1 with variation in B.

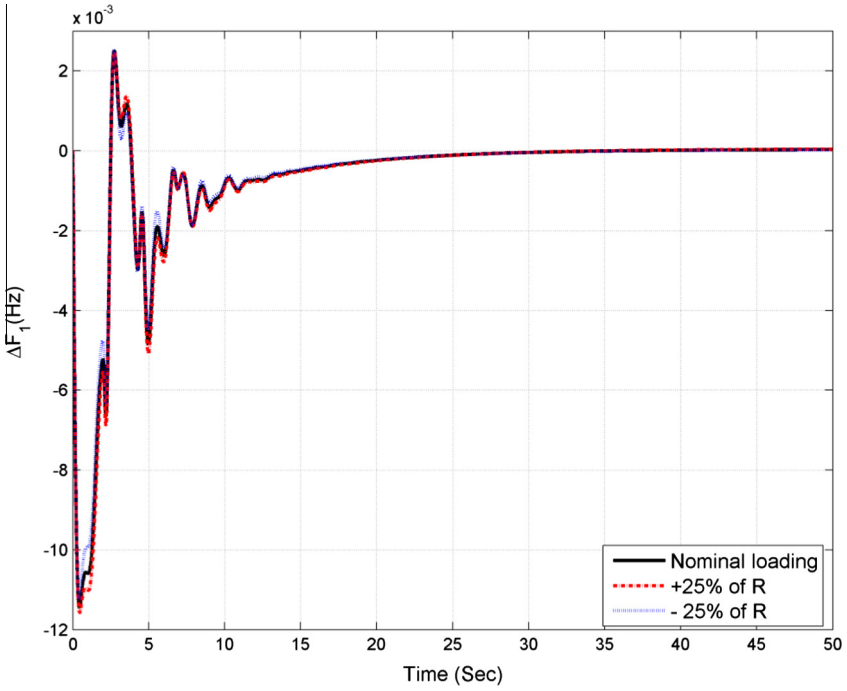

Figure 19 Change in frequency of area-1 for 1% load change in area-1 with variation in R.

(ii) **TCSC data**

$T_{12} = 0.0866;\ \delta_0 = 300;\ X_t = 10$ p.u.; $K_{TCSC} = 2.0;$
$T_{TCSC} = 0.02$ s

(iii) **SMES data**

$K_{SMES} = 0.12;\ T_{SMES} = 0.03$ s

References

[1] Kundur P. Power system stability and control. New York: McGraw-Hill; 1994.
[2] Elgerd OI. Electric energy systems theory – an introduction. 2nd ed. Tata McGraw Hill; 2007.
[3] Kothari DP, Nagrath IJ. Modern power system analysis. 4th ed. New Delhi: Tata McGraw-Hill; 2011.
[4] Saikia LC, Nanda J, Mishra S. Performance comparison of several classical controllers in AGC for multi-area interconnected thermal system. Int J Electr Power Energy Syst 2011;33:394–401.
[5] Parmar KPS, Majhi S, Kothari DP. Load frequency control of a realistic power system with multi-source power generation. Int J Electr Power Energy Syst 2012;42:426–33.
[6] Saikia LC, Mishra S, Sinha N, Nanda J. Automatic generation control of a multi area ydrothermal system using reinforced learning neural network controller. Int J Electr Power Energy Syst 2011;33(4):1101–8.
[7] Ibraheem KP, Kothari DP. Recent philosophies of automatic generation control strategies in power systems. IEEE Trans Power Syst 2005;20(1):346–57.
[8] Ghosal SP. Optimization of PID gains by particle swarm optimization in fuzzy based automatic generation control. Electr Power Syst Res 2004;72(3):203–12.
[9] Golpira H, Bevrani H, Golpira H. Application of GA optimization for automatic generation control design in an interconnected power system. Energy Convers Manage 2011;52:2247–55.
[10] Yesil E, Guzelkaya M, Eksin I. Self tuning fuzzy PID type load and frequency controller. Energy Convers Manage 2004;45(3):377–90.
[11] Khuntia SR, Panda S. Simulation study for automatic generation control of a multi-area power system by ANFIS approach. Appl Soft Comput 2012;12(1):333–41.
[12] Hingorani NG, Gyugyi L. Understanding FACTS-concepts and technology of flexible AC transmission systems. Standard Publishers, IEEE Press; 2000.
[13] Praghnesh B, Ghoshal SP, Ranjit R. Load frequency stabilization by coordinated control of thyristor controlled phase shifters and superconducting magnetic energy storage for three types of interconnected two-area power systems. Int J Electr Power Energy Syst 2010;32:1111–24.
[14] Mathur RM, Varma RK. Thyristor-based FACTS controllers for electrical transmission systems. IEEE Press, John Wiley & Sons, inc. publication; 2002.
[15] Stron R, Price K. Differential evolution – a simple and efficient adaptive scheme for global optimization over continuous spaces. J Global Optim 1995;11:341–59.
[16] Das S, Suganthan PN. Differential evolution: a survey of the state-of-the-art. IEEE Trans Evol Comput 2011;15:4–31.
[17] Brest J, Greiner S, Boskovic B, Mernik M, Zumer V. Self-adapting control parameters in differential evolution: a comparative study on numerical benchmark problems. IEEE Trans Evol Comput 2005;10:646–57.
[18] Cheres E. The application of generation rate constraint in modeling of a thermal power system. Electr Power Comp Syst 2001;29(2):83–7.
[19] Ignacio E, Fernandez-Bernal F, Rouco L, Elosia P, Saiz-Chicharro A. Modeling of thermal generating units for automatic

generation control purposes. IEEE Trans Control Syst Technol 2004;12(1):205–10.
[20] Panda S. Differential evolution algorithm for SSSC-based damping controller design considering time delay. J. Franklin Inst 2011;348(8):1903–26.
[21] Mudi KR, Pal RN. A robust self-tuning scheme for PI-and PD-type fuzzy controllers. IEEE Trans Fuzzy Syst 1999;7(1):2–16.
[22] Woo WZ, Chung YH, Lin JJ. A PID type fuzzy controller with self tuning scaling factors. Fuzzy Sets Syst 2000;115(2):321–6.
[23] Shabani H, Vahidi B, Ebrahimpour M. A robust PID controller based on imperialist competitive algorithm for load–frequency control of power systems. ISA Trans. 2012;52:88–95.
[24] Sudha KR, Vijaya SR. Load frequency control of an interconnected reheat thermal system using type-2 fuzzy system including SMES units. Int J Electr Power Energy Syst 2012;43:1383–92.
[25] Janez B, Saso G, Borko B, Marjan M, Viljem Z. Self-adapting control parameters in differential evolution: a comparative study on numerical benchmark problems. IEEE Trans Evol Comput 2005;10:646–57.
[26] Qin AK, Huang VL, Suganthan PN. Differential evolution algorithm with strategy adaptation for global numerical optimization. IEEE Trans Evol Comput 2009;13:398–417.
[27] Sahu RK, Panda S, Rout UK. DE optimized parallel 2-DOF PID controller for load frequency control of power system with governor dead-band nonlinearity. Int J Electr Power Energy Syst 2013;49:19–33.
[28] Rout UK, Sahu RK, Panda S. Design and analysis of differential evolution algorithm based automatic generation control for interconnected power system. Ain Shams Eng J 2013;4(3):409–21.

Saroj Padhan is received the Master's degrees in Electrical Engineering in 2012 from Veer Surendrai Sai University of Technology (VSSUT), Burla, Odisha, India. He is currently working towards the Ph.D. degree at the Department of Electrical Engineering, VSSUT, Burla, Odisha, India. His research interests include automatic generation control and optimization techniques.

Rabindra Kumar Sahu received the Ph.D. degree from the Indian Institute of Technology Madras, in 2007. He is currently working as Reader in the Department of Electrical Engineering, Veer Surendrai Sai University of Technology (VSSUT), Burla, Sambalpur, Odisha, India. His research interests include application of soft computing techniques to power system engineering, Flexible AC Transmission Systems (FACTS). Dr. Sahu is life member of ISTE.

Sidhartha Panda received Ph.D. degree from Indian Institute of Technology (IIT), Roorkee, India, M.E. degree from Veer Surendrai Sai University of Technology (VSSUT). Presently, he is working as a Professor in the Department of Electrical Engineering, Veer Surendrai Sai University of Technology (VSSUT), Burla, Sambalpur, Odisha, India. His areas of research include Flexible AC Transmission Systems (FACTS), Power System Stability, Soft computing, Model Order Reduction, Distributed Generation and Wind Energy. Dr. Panda is a Fellow of Institution of Engineers (India).